AIP | Journal of Applied Physics

Al doped ZnO nanoplate arrays and microbox structures grown by thermal deposition

Y. Ortega, P. Fernández, and J. Piqueras

Citation: J. Appl. Phys. 105, 054315 (2009); doi: 10.1063/1.3079523
View online: http://dx.doi.org/10.1063/1.3079523
View Table of Contents: http://jap.aip.org/resource/1/JAPIAU/v105/i5
Published by the AIP Publishing LLC.

Al doped ZnO nanoplate arrays and microbox structures grown by thermal deposition

Y. Ortega,[a] P. Fernández, and J. Piqueras
Departamento de Física de Materiales, Facultad de Ciencias Físicas, Universidad Complutense de Madrid, 28040 Madrid, Spain

(Received 11 October 2008; accepted 6 January 2009; published online 13 March 2009)

Al doped ZnO arrays of nanoplates and of ordered nanoneedles have been grown by a thermal evaporation-deposition method. The nanoplates, which have mainly triangular shape. Interpenetrating triangles and crossing of the triangles with other planar arrangements form a structure consisting of arrays of microboxes. The influence of Al on the luminescence of the nanostructures has been studied by cathodoluminescence (CL) in the scanning electron microscope. Intense CL emission from the internal faces of the microboxes is related to the presence of deep level defects. © *2009 American Institute of Physics*. [DOI: 10.1063/1.3079523]

I. INTRODUCTION

Doping of ZnO with elements such as Al, Ga, In, Sn, or Ge produces an increase in electrical conductivity which is of interest for different potential applications of this material.[1–4] In particular, Al doped ZnO shows a high conductivity without loss of the good optical transmission properties of pure ZnO in the visible and the near infrared ranges. For this reason ZnO:Al is considered as a suitable material, comparable to indium tin oxide compounds, for applications as transparent conductor. Most of the studies on Al doped ZnO deal with structural, electrical, and optical properties of thin films grown by methods such as sol-gel[3,4] sputtering[5–8] or spray pyrolysis,[9] but there are few reports on elongated nanostructures. The increasing interest in one-dimensional nanostructures of doped ZnO to obtain structures with improved optical or electrical properties has lead to the synthesis of ZnO nanowires or nanobelts doped with Sn,[10,11] In,[12,13] Ga,[14] Mn,[15] and other elements. There are few reports on Al doped nanostructures. ZnO:Al microrods[16] and nanorods[17] have been grown by a thermal evaporation method; nanowires and nanotubes have been obtained by alloy evaporation-deposition;[18] and nanocones and other nanostructures have been grown by pulsed laser deposition.[19] In the present work ZnO:Al nanoneedles and different arrays of planar nanostructures have been grown by thermally treating a compacted mixture of ZnO and Al_2O_3 powders under argon flow. This method has been reported to lead to the growth of elongated nanostructures or nanoplates of oxides such as ZnO,[11,20] In_2O_3,[21] Ga_2O_3,[22] GeO_2,[23] or V_2O_5.[24] The obtained Al doped nanostructures have been characterized by x-ray diffraction (XRD), scanning electron microscopy (SEM), x-ray energy dispersive spectroscopy (EDS) in SEM, cathodoluminescence (CL) in SEM, and transmission electron microscopy (TEM).

II. EXPERIMENTAL METHOD

The starting materials used were ZnO and Al_2O_3 powders with purities of 99.999% and 99.9%, respectively. $ZnO-Al_2O_3$ mixtures with 1, 5, and 10 wt. % of Al_2O_3, respectively, were prepared by milling the corresponding powders in a centrifugal ball mill (Retsch S100) with 20 mm agate balls for 5 h. The mixture was then compacted under a compressive load to form disk shaped samples of about 7 mm diameter and 2 mm thickness. As described below, these treatments lead to the growth of microstructures and nanostructures on the sample surface. By annealing at lower temperatures or with shorter times no structures were grown, while at higher temperatures no substantial changes were observed as compared with the 1280 °C treatments. The samples were then annealed at 1280 °C for 15 h under argon flow. XRD measurements were performed with a Philips diffractometer. Secondary electron and CL observations were carried out in a Leica 440 SEM, a Hitachi S2500 SEM, and a FEI Inspect SEM. The CL measurements were carried out at liquid nitrogen temperature with a Hamamatsu R928 photomultiplier or a PMA-11 charge coupled device camera. Energy dispersive x-ray microanalysis was performed in a Leica 440 SEM with a Bruker AXS Quantax system working at 20 keV and 5 nA. TEM, high-resolution TEM (HRTEM), and selected area electron diffraction (SAED) analyses were performed with JEOL JEM 2000FX and JEM 3000F microscopes.

III. RESULTS AND DISCUSSION

After the thermal treatments at 1280 °C, microstructures and nanostructures, whose morphologies depend on the composition of the initial powder mixture, were grown on the sample surface. In all samples prepared with powders containing 1 or 5 wt. % Al, both microrods with rough lateral surfaces and pencil-like rods with prismatic shapes are observed (Fig. 1). Such structures are similar to those obtained by the same thermal method when pure ZnO powder is used as starting material[20] and were not further investigated. A higher Al content (10 wt. %) in the precursor leads to nanostructures with a morphology consisting of complex arrays of nanoneedles and nanoplates with well defined geometry. Figure 2(a) shows a long structure with a core formed by arrays of interpenetrating triangles and a high number of well

[a]E-mail: yanicet@fis.ucm.es.

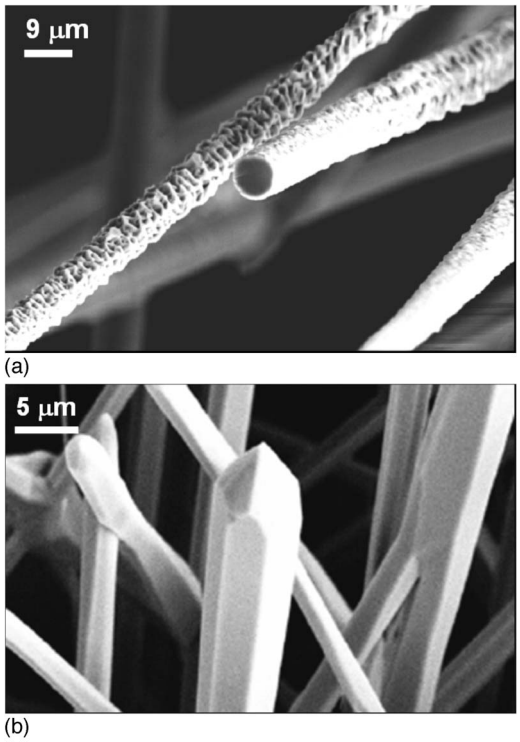

FIG. 1. Microstructures of Al-doped ZnO (a) microrods with rough lateral surfaces and (b) pencil-like rods with prismatic shapes.

aligned nanoneedles which grow at two sides of the core, perpendicular to the growth axis. Figure 2(b) shows a side view of the core structure in which a distribution of cavities, resulting of the intersection of triangles and other plates, is observed. Arrays of ZnO nanoneedles grown at two opposite $[000\bar{1}]$ faces of a nanoplate have been previously reported.[20,25] The growth takes place preferentially at one side of the plate because the oxygen terminated surface yield a lower growth ratio than the Zn terminated surface.[25]

Triangular shaped ZnO nanoblades, grown by vapor deposition of $ZnO-SnO_2$ powders, have been described to form the so called nanopropellers[26] consisting of blades with sixfold symmetry around a central wire. The blades of the nanopropeller had isosceles triangular shape with a small Sn particle at the tip which indicates a vapor-liquid-solid (VLS) growth mechanism. The growth direction of the nanoblade was found to be [2110]. Also ZnO triangular nanoplates with $[01\bar{1}0]$ growth direction have been grown on a Si substrate with Au catalyst.[27]

The triangles observed in this work only grow in the samples with higher Al content in the precursor, which suggests that their formation is associated to the presence of Al. No triangles were found in undoped[20] or Sn doped[11] ZnO microstructures grown by the same procedure used here. EDS measurements show that Al content in the triangles is about 10 at. %, while Al content in the nanoneedles is about 1 at. %. The Al content in the rods grown from powders with 5 wt. % Al_2O_3, as that shown in Fig. 1, is in the range 1–2 at. %.

XRD of the treated samples show that the disk substrates contain ZnO and $ZnAl_2O_4$ phases but the grown structures consist only of the hexagonal ZnO phase. Figure 3 shows the

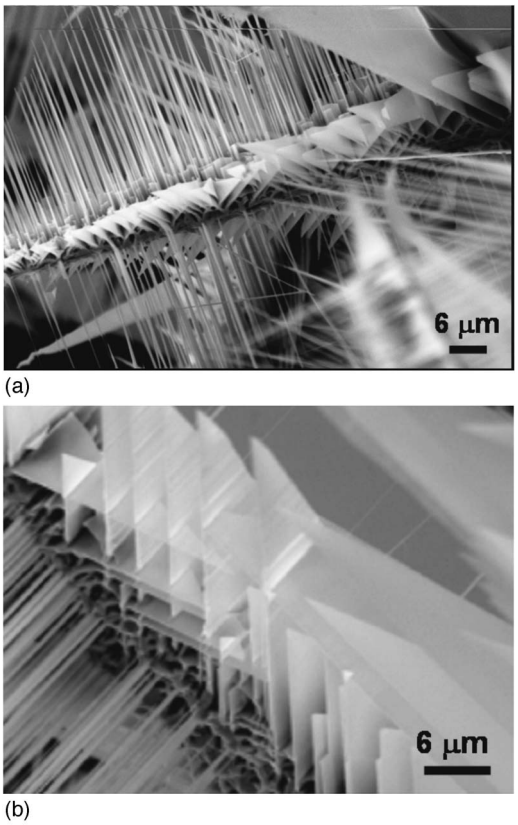

FIG. 2. (a) Al-doped ZnO long structure with a core formed by arrays of interpenetrating triangles and a high number of well aligned nanoneedles. (b) A side view of the core structure showing a distribution of cavities.

XRD pattern of the structures showing preferred (103) orientation, different to the (002) orientation reported for aligned Al doped microrods[16] or the (201) orientation of triangular undoped nanoplates.[27] Selected area diffraction patterns and TEM images of the nanostructures reveal their single-crystalline nature. Figure 4(a) shows the TEM image of a nanotriangle and the corresponding diffraction pattern. HRTEM of the needles [Fig. 4(b)] reveals a wavy edge and lattice fringes perpendicular to the edge of the needle. The spacing of the fringes, 0.26 nm, corresponds to the (002) planes, showing that the growth axis of the needles is [001].

It was tentatively suggested in Ref. 27 that for the

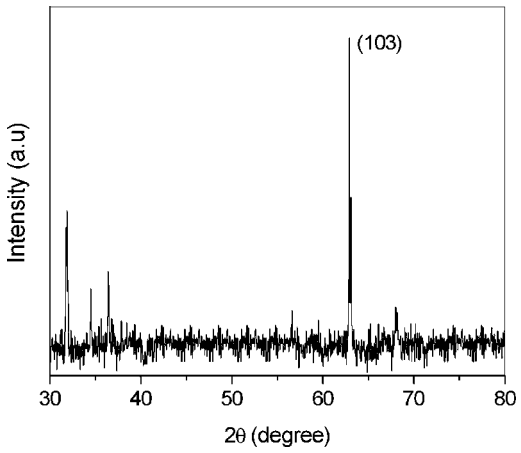

FIG. 3. XRD pattern of the structures shown in Fig. 2.

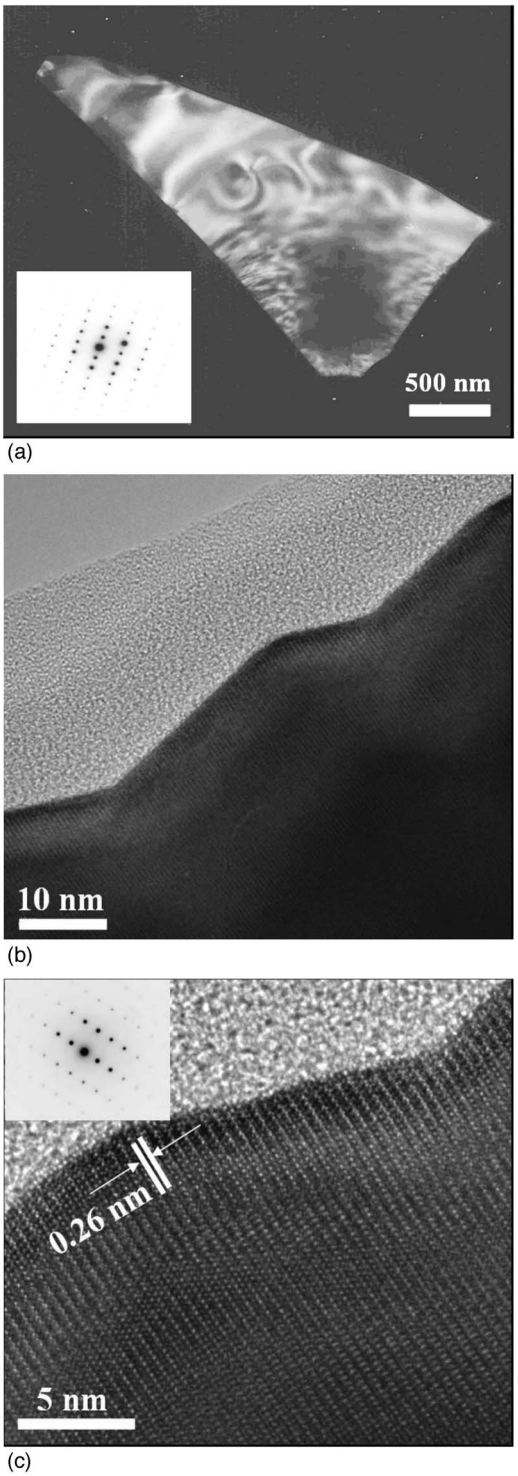

FIG. 4. (a) TEM image of a nanotriangle and the corresponding diffraction pattern. (b, c) HRTEM of a needle and the corresponding diffraction pattern.

growth of the ZnO nanotriangles, the Zn vapor concentration should be very low and decrease with time. This condition is related to the reduction in ZnO nanopowders by Ga and does not apply to this work. In Ref. 26 it was reported that the morphology of the triangular blades depends on the local temperature and availability of Zn-O vapor so that in a certain temperature range there is transverse growth which extends the width of the nanoblades as the growth along ⟨2110⟩ proceeds resulting in the formation of triangular blades. At

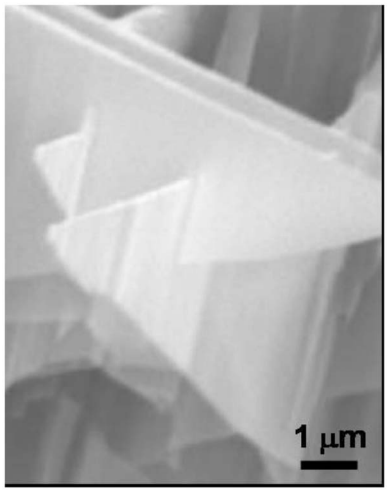

FIG. 5. SEM image of partially crossing triangles.

higher temperatures there is a faster directional growth and longer nanoblades are formed. In our case, with a uniform temperature in the sample, the parameter determining the formation of the triangles is the presence of Al. We suggest that a high Al content retards a directional growth and favors the transverse growth and the consequent formation of triangles. This process takes place only when a high Al content, in this case about 10 at. %, is incorporated into the structure, while needle-shape structures with a high directional growth contain only about 1 at. % of Al. Also Tang *et al.*[16] obtained undoped and Al (0.7 at. %) doped ZnO similar microrods by a thermal evaporation method. Undoped (20) and Sn (under 1 at %) doped[11] ZnO nanostructures grown by the same method and under similar experimental conditions used here, did not show the triangular morphology. The influence of Al on the morphology of the nanostructures depends on the growth method and the specific growth parameters used. For instance, in Ref. 18 ZnO:Al nanotubes with 12 at. % Al were grown by chemical vapor deposition at low temperature and no triangles were reported showing that morphology does not simply depend on Al doping.

One striking feature of the triangle arrays is their perfect interpenetration, shown in Fig. 2(b), which takes place without change in shape or growth direction. A model of interpenetration of ZnO nanorods has been proposed[28] in which longitudinal and transverse growths lead to the joining of the rods. SEM observations of the triangle arrays do not enable to determine the growth mechanism and how the interpenetration takes place. Partially crossing triangles have been occasionally observed, Fig. 5, which could indicate that in some cases longitudinal and transverse growths take place. Single arrays of parallel triangles are also observed to grow on planar structures (Fig. 6). Crossing of arrays of triangles or crossing of triangles with other planar structures form a ZnO microbox structure which is shown at high magnification in Fig. 7. Triangular ZnO nanoplates are considered of interest as field emitters because of their large field enhancement factor and the large surface area for heat dissipation which leads to very stable and low-threshold field

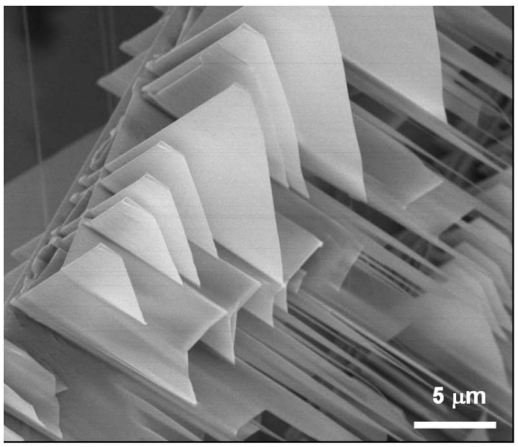

FIG. 6. (Color online) Single arrays of parallel triangles.

emission.[27] The geometry of the structures obtained in this work, forming arrays of empty boxes, would also favors heat dissipation.

Al doping of ZnO has been reported to induce an increase in carrier concentration and a broadening of the optical band gap which has been sometimes explained in terms of the Burstein-Moss effect due to the Fermi level moving into the conduction band.[8,29] The gap widening is revealed by a shift in the absorption band edge[8,17,29,30] and by the

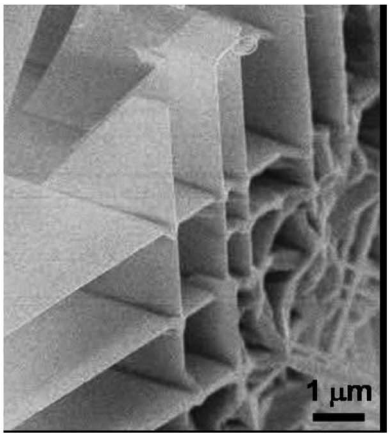

(a)

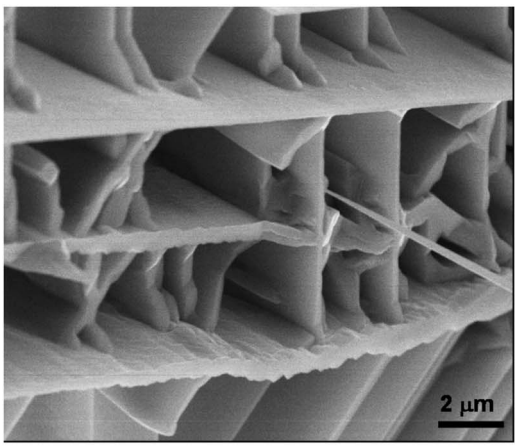

(b)

FIG. 7. Al-doped ZnO microbox structure formed (a) by crossing of arrays of triangles (b) or by crossing of triangles with other planar structures.

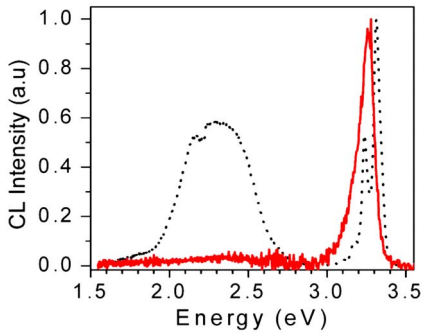

FIG. 8. (Color online) CL spectra of undoped ZnO (solid line) and of the Al doped (dotted line) nanostructures.

corresponding blueshift of the near band edge emission energy in luminescence spectra.[17,18,30] The blueshift values do not appear to show a clear correspondence with the Al concentration in the samples. In Ref. 18, a blueshift of the near band edge CL emission to 3.34 eV was found in 2.5 at. % Al doped nanowires, compared with 3.29 eV from undoped ZnO nanowires. However, no further blueshift was detected in nanowire/nanotube junctions containing 12 at. % Al. A blueshift of the photoluminescence band edge emission was observed in Ref. 31 up to 5 at. % Al in ZnO films. Suchea *et al.*[8] reported a blueshift from 3.31 to 3.35 eV in their films which was much smaller than predicted from Burstein-Moss theory at 2 at. % Al doped films. CL spectra of undoped ZnO and of the Al doped nanostructures of this work (Fig. 8) show a blueshift from 3.26 eV to about 3.31 eV. Measurements performed in regions with different Al content, as triangles and nanoneedles, did not reveal a correspondence between the amount of blueshift and the Al content as measured by EDS, similar to the observation of Ref. 18.

CL images reveal that the internal part of the microboxes emit with higher intensity than the external faces or other planar features of the sample (Fig. 9). This is due to the defect structure resulting from the growth process. CL spectra recorded inside and outside the boxes [Fig. 9(c)] show that the enhanced luminescence in the interior is mainly due to the higher intensity of the defect related green band, which is known to have a contribution of the oxygen vacancy related defects.

IV. CONCLUSIONS

Al doped ZnO nanostructures and microstructures, mainly arrays of triangular nanoplates and of ordered nanoneedles, have been obtained by thermal treatment of compacted mixtures of ZnO and Al_2O_3 powders. Interpenetrating triangles and crossing of triangles with other nanoplates form a structure consisting of arrays of microboxes with wall thicknesses of few hundreds of nanometers. The geometry of interpenetrating Al doped plates would be favorable for applications, such as field emission, in which heat dissipation is of interest. Al doping causes a blueshift of the near band edge CL emission of ZnO. However, the blueshift observed in the structures, typically of about 50 meV, could not be correlated with the local Al content as measured by EDS. CL measurements show an enhanced luminescence from the in-

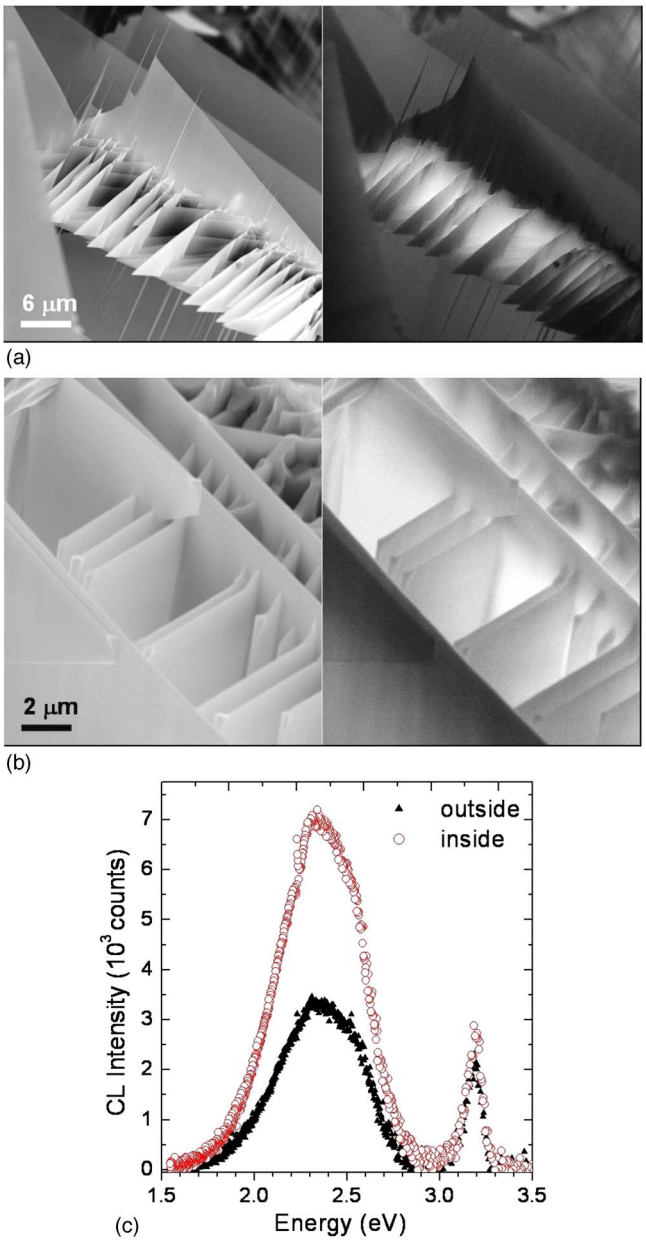

FIG. 9. (Color online) SEM and CL images of an array of (a) triangles and (b) microboxes. (c) CL spectra recorded outside and inside the boxes.

ternal faces of the microboxes, as compared with other planar regions, which is due to the enhanced intensity of defect green band.

ACKNOWLEDGMENT

This work was supported by MEC (Project No. MAT2006-01259).

[1]R. Wang, L. H. King, and A. W. Sleight, J. Mater. Res. **11**, 1659 (1996).
[2]M. Chen, Z. L. Pei, X. Wang, C. Sun, and L. S. Wen, J. Vac. Sci. Technol. A **19**, 963 (2001).
[3]J. H. Lee and B. O. Park, Thin Solid Films **426**, 94 (2003).
[4]H. M. Zhou, D. Q. Yi, Z. M. Yu, L. R. Xiao, and J. Li, Thin Solid Films **515**, 6909 (2007).
[5]J. Y. Hwang, C. R. Cho, S. A. Lee, and S. Y. Jeong, J. Korean Phys. Soc. **47**, S228 (2005).
[6]K. Yim and C. Lee, Cryst. Res. Technol. **41**, 1198 (2006).
[7]D. Horwat and A. Billard, Thin Solid Films **515**, 5444 (2007).
[8]M. Suchea, S. Christoulakis, N. Karsarakis, T. Kitsopoulos, and G. Kirikiadis, Thin Solid Films **515**, 6562 (2007).
[9]M. Caglar, S. Ilican, Y. Caglar, and F. Yakuphanoglu, J. Mater. Sci.: Mater. Electron. **19**, 704 (2008).
[10]S. Y. Li, P. Lin, C. Y. Lee, T. Y. Tseng, and C. J. Huang, J. Phys. D **37**, 2274 (2004).
[11]Y. Ortega, P. Fernández, and J. Piqueras, Nanotechnology **18**, 115606 (2007).
[12]J. G. Wen, J. Y. Lao, D. Z. Wang, T. M. Kyaw, Y. L. Foo, and Z. F. Ren, Chem. Phys. Lett. **372**, 717 (2003).
[13]L. Xu, Y. Xu, Y. Chen, H. Xiao, L. Zhu, Q. Zhou, and S. Li, J. Phys. Chem. B **110**, 6637 (2006).
[14]C. X. Xu, X. W. Sun, and B. J. Chen, Appl. Phys. Lett. **84**, 1540 (2004).
[15]C. Ronning, P. X. Gao, Y. Ding, Z. L. Wang, and D. Schwen, Appl. Phys. Lett. **84**, 783 (2004).
[16]H. Tang, L. Zhu, H. He, Z. Ye, Y. Zhang, M. Zhi, Z. Yang, B. Zhao, and T. Li, J. Phys. D **39**, 2696 (2006).
[17]H. P. He, H. P. Tang, Z. Z. Ye, L. P. Zhu, B. H. Zhao, L. Wang, and X. H. Li Appl. Phys. Lett. **90**, 023104 (2007).
[18]R. Wang, C. Liu, J. Huang, and S. Chen, Appl. Phys. Lett. **88**, 023111 (2006).
[19]Y. Sun, K. E. Addison, and M. N. R. Ashfold, Nanotechnology **18**, 495601 (2007).
[20]J. Grym, P. Fernández, and J. Piqueras, Nanotechnology **16**, 931 (2005).
[21]D. A. Magdas, A. Cremades, and J. Piqueras, Appl. Phys. Lett. **88**, 113107 (2006).
[22]E. Nogales, B. Méndez, and J. Piqueras, Appl. Phys. Lett. **86**, 113112 (2005).
[23]P. Hidalgo, B. Méndez, and J. Piqueras, Nanotechnology **16**, 2521 (2005).
[24]C. Díaz-Guerra and J. Piqueras, J. Appl. Phys. **102**, 084307 (2007).
[25]Z. L. Wang, X. Y. Kong, and J. M. Zuo, Phys. Rev. Lett. **91**, 185502 (2003).
[26]P. X. Gao and Z. L. Wang, Appl. Phys. Lett. **84**, 2883 (2004).
[27]P. Feng X. Q. Fu, S. Q. Li, Y. G. Wang, and T. H. Wang, Nanotechnology **18**, 165704 (2007).
[28]R. Yang and Z. L. Wang, Solid State Commun. **134**, 741 (2005).
[29]M. K. Jayaraj, A. Antony, and M. Ramachandran, Bull. Mater. Sci. **25**, 227 (2002).
[30]H. W. Lee, S. P. Lau, Y. G. Wang, K. Y. Tse, H. H. Hng, and B. K. Tay, J. Cryst. Growth **268**, 596 (2004).
[31]C. D. Bojorge, H. R. Cánepa, U. E. Gilabert, D. Silva, E. A. Dalchiele, and R. E. Marotti, J. Mater. Sci.: Mater. Electron. **18**, 1119 (2007).